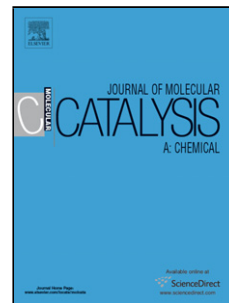


## Accepted Manuscript

Title: The enantioselectivity of the manganese-salen complex in the epoxidation of unfunctionalized olefins and the influence of grafting

Author: Thomas Bogaerts Sebastian Wouters Pascal Van Der Voort Veronique Van Speybroeck



PII: S1381-1169(15)00204-6  
DOI: <http://dx.doi.org/doi:10.1016/j.molcata.2015.05.020>  
Reference: MOLCAA 9506

To appear in: *Journal of Molecular Catalysis A: Chemical*

Received date: 4-11-2014  
Revised date: 2-5-2015  
Accepted date: 25-5-2015

Please cite this article as: Thomas Bogaerts, Sebastian Wouters, Pascal Van Der Voort, Veronique Van Speybroeck, The enantioselectivity of the manganese-salen complex in the epoxidation of unfunctionalized olefins and the influence of grafting, *Journal of Molecular Catalysis A: Chemical* <http://dx.doi.org/10.1016/j.molcata.2015.05.020>

This is a PDF file of an unedited manuscript that has been accepted for publication. As a service to our customers we are providing this early version of the manuscript. The manuscript will undergo copyediting, typesetting, and review of the resulting proof before it is published in its final form. Please note that during the production process errors may be discovered which could affect the content, and all legal disclaimers that apply to the journal pertain.

## The enantioselectivity of the manganese-salen complex in the epoxidation of unfunctionalized olefins and the influence of grafting

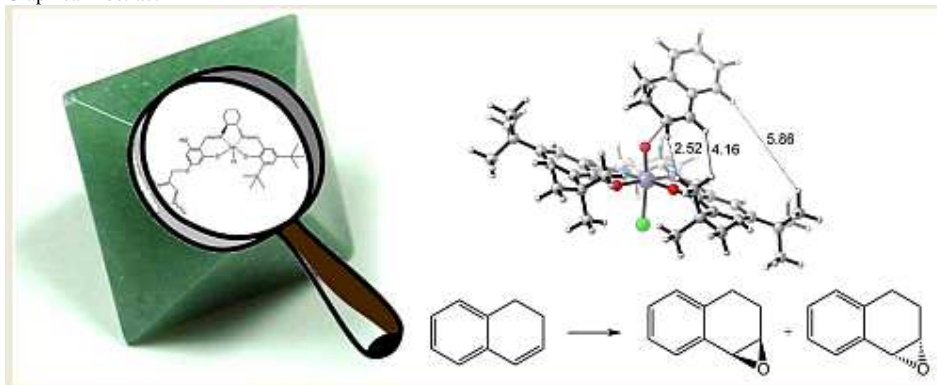
Thomas Bogaerts<sup>a,b</sup>, Sebastian Wouters<sup>a</sup>, Pascal Van Der Voort<sup>b</sup>\*[pascal.vandervoort@ugent.be](mailto:pascal.vandervoort@ugent.be), Veronique Van Speybroeck<sup>a</sup>\*[Veronique.vanspeybroeck@ugent.be](mailto:Veronique.vanspeybroeck@ugent.be)

<sup>a</sup>Center for Molecular Modelling (CMM), Ghent university, Technologiepark 903, 9052 Zwijnaarde

<sup>b</sup>Center for Ordered Materials, Organometallics and Catalysis (COMOC), Department of Inorganic and Physical Chemistry, Ghent University, Krijgslaan 281-S3, 9000 Ghent, Belgium

\*Corresponding author.

Graphical Abstract



## Highlights

- Ab initio modelling of the influence of grafting of manganese-salen complexes.
- Asymmetric salen complexes exhibit reduced enantioselectivity.
- Asymmetric complex grafted to a metal organic framework via a stepwise procedure.
- A catalytic test shows the decrease in selectivity is limited, the MIL-101(Cr) structure is a good support.

*Jacobsen's complexes are famous for their usability for enantioselective epoxidations. However, the applicability of this catalytic system has been severely limited by several practical problems such as deactivation and separation after reaction. Grafting of Jacobsen-type complexes on solid supports is an attractive way to overcome these problems but led to a decrease in selectivity. A combined theoretical and experimental approach is presented to unravel the factors governing enantioselectivity. The importance of different substituents was determined by analyzing the transition state for the oxygen transfer using the full system as a model. An analysis of the asymmetric complex has shown an inherent tendency for a decreased selectivity due to the lack of specific bulky groups. Experimentally an immobilized Jacobsen catalyst on a metal organic framework (MIL-101) was synthesized which confirms the computational tendencies but the decrease in selectivity is limited, indicating that the MIL-101(Cr) is a suitable carrier for this complex.*

**Keywords:** ab initio modelling; metal organic frameworks; enantioselective catalysis; heterogeneous catalysis

## 1. Introduction

Reactive chiral products are of great value in the chemical industry<sup>1-3</sup>. Many commercial products contain some sort of chiral center and the production of these can be facilitated by readily accessible chiral intermediates. One compound that can serve as such an intermediate is a chiral epoxide. These compounds are very reactive due to the epoxide ring and the chirality can be transferred to further products.

Given the synthetic value of chiral epoxides many catalytic systems have been developed to produce these compounds with high selectivity, with the titanium tartrate catalyst<sup>4-10</sup> and the chiral metal-salen complex<sup>11-16</sup> as the most well-known. The latter complexes, originally designed by Jacobsen and Katsuki, are highly performant in the epoxidation of unfunctionalized olefins. With optimized conditions, olefins such as styrene<sup>16</sup> and chromene derivatives<sup>14</sup> could be epoxidized with high (>85% ee) selectivities. Different oxidizing agents can be applied with the catalytic system, for example NaOCl in aqueous media or meta-chloroperoxybenzoic acid in organic solvents.

Despite their large applicability and commercial availability the mechanism that controls the enantioselectivity is not thoroughly understood. Several experiments have been conducted to probe the approach vectors<sup>13,14,17</sup> (Table 1). From a computational approach numerous ab initio studies on the mechanism of oxygen transfer using a smaller model for the Jacobsen catalyst<sup>18-21</sup> have been performed. Linde *et al.*<sup>22,23</sup> acknowledged early on that the choice of a different spin state (spin 0, 1 or 2) has a huge influence on the resulting reaction mechanism. They proposed the existence of different intermediates depending on the spin state of the complex. Cavallo *et al.*<sup>24,25</sup> further investigated this phenomenon and noticed the importance of the choice of the right DFT functional. Their research allowed for the proposition of a catalytic cycle for the epoxidation using sodium hypochlorite<sup>20</sup>. However next to these studies on the mechanism of oxygen transfer, the research on the selectivity has always been performed with molecular mechanics methods<sup>19</sup>. To obtain a full understanding of all interactions contributing to the overall selectivity it is recommended to model the complete catalyst at a higher level of theory. Such studies have now become feasible with current computational resources.

Experiments with styrene derivatives featuring different substituents<sup>17</sup> have led to the conclusion that the so called distal, side-on approach (schematically shown in *Figure 1*), where the substrate approaches from the side and the most bulky group is pointed away from the complex is preferred, except for some tri-substituted variants. However, an experiment where different substituents were introduced on the salen ligand<sup>14</sup> seemed to point to an approach via the backbone (diamine). The molecular mechanics study allowed to identify different possibilities for the approach but, due the use of classical force fields, no transition states could be considered. Therefore no conclusion on the influence of the transition state on the selectivity could be drawn. Regardless of these previous studies, the most important feature of a salen type complex with a diaminocyclohexane backbone appear to be the substituents on the 3/3' positions as schematically shown in *Figure 2*. In the

absence of bulky groups at these positions all selectivity is inhibited<sup>13</sup>. The substituents on the 5/5' positions<sup>14</sup> also have an influence on the resulting selectivity but the above mentioned studies could not provide a rationale for this observation

In this paper we provide an in depth study on the selectivity of the salen complex by localizing the transition states of various approach modes using a density functional theory (DFT) methodology in which the full catalyst complex is taken into account. This is, to our knowledge, the first time a DFT methodology is applied on the Jacobsen complex without simplification of the complex by omitting functional groups or larger parts of the complex. A report by Morokuma *et al.*<sup>26</sup> already showed the importance of including the salicylaldehyde parts in the model, but the inclusion of functional groups on these moieties will further improve the results. Both symmetrical and asymmetrical salen complexes will be investigated to get an in-depth view on the effect of substituents at various positions of the ligands on the selectivity. This is important when considering the effect of the covalent grafting of salen-type complexes, where an asymmetric substitution is often used to bind the complex to a support<sup>27-29</sup>. Such grafting procedures, or in general the immobilization of the homogeneous system into a heterogeneous system might be beneficial. Similar to many other homogeneous catalysts, the separation of the complex after reaction is a significant bottleneck its applicability. Moreover, manganese-salen type complexes undergo deactivation via an irreversible stacking of the oxidized species, impeding their long-term use. The most effective way to optimize the catalyst is the immobilization of the homogeneous system on a solid support that impedes any stacking and facilitates the separation of the catalyst. On the other hand care needs to be taken in how far such procedure maintains the original high selectivity of the homogeneous system. In an earlier study<sup>30</sup> of the present authors a heterogeneous system was developed by the encapsulation of the Jacobsen complex in the pores of a metal organic framework. This immobilization omitting all covalent bonds, resulting in a material that maintained the selectivity of the original catalyst. This could be explained by simulations of the epoxidation reaction where it was shown that the transition state governing the selectivity fitted perfectly in the cage of the host structure.

In this study we will assess the effect of a grafting procedure of the salen complex on its selectivity. The host material for the grafting procedure is the metal organic framework (MOF) MIL-101<sup>31,32</sup>. This material has been chosen for the high stability in the various media that are used in the postmodification process. There have been various studies where the salen complex was immobilized on different supports<sup>28,29,33-35</sup>. This mostly led to a decrease in selectivity unless there was no covalent interaction between the complex and the host, allowing a high freedom of movement<sup>30</sup>. One possible approach to immobilizing the complex is building it up piece by piece on the solid support, as reported by Angelino *et al.*<sup>28,29</sup> In this paper a similar approach is used anchoring the catalyst on a chloromethylated MIL-101.

## 2. Computational and experimental methods

### 2.1. Reaction mechanism and models used for the catalyst

In an earlier study we have proven that by using the full salen complex as a model (*Figure 3 (a)*) the different approach vectors leading to the various enantiomers could be found. In addition, the difference in free energies between the various transition states were able to explain the observed

selectivity of the catalyst.<sup>30</sup> In order to obtain a sufficient amount of detail, the full catalyst was used as a model, since any simplification would risk the loss of critical information on the steric influence. It was also shown that the calculations on the homogeneous system were able to rationalize also the observed selectivities for the same catalyst which was embedded in the NH<sub>2</sub>-MIL-101(Al) system. In this paper we use the same model system for the computational study but both symmetric and asymmetric salen complexes have been considered to get insight into the effect of grafting on the selectivity. Indeed, a grafting procedure always disrupts the symmetry in the ligand system. All considered systems are shown in Figure 3. Model (a) represents the symmetric salen complex which is taken as the reference system. Model (b) consists of a 2,4,6-trihydroxybenzaldehyde moiety at one side and 3,5-di-tert-butylbenzaldehyde at the other side. Model (c) has a methylbenzene substituted on one of the hydroxyl groups to mimic the grafting.

Early after the discovery of the salen ligands and their usefulness in selective epoxidation reactions the Mn<sup>V</sup>=O species was identified as a plausible intermediate<sup>36,37</sup>. Starting from the oxidized form of the complex the epoxide is formed in a two-step reaction, in the first step a single oxygen-carbon bond is formed leading to a radical intermediate, as shown in the mechanism in figure S3 of the supporting information. Afterwards this intermediate loses its radical character by forming the epoxide, this mechanism has been supported by the previous computational studies<sup>20</sup>. It has been proposed that this reaction can take place in different spin states, spin 0,1 or 2<sup>38</sup>. A detailed study of the spin states of oxidized complexes was reported before<sup>39</sup>. The step where the first carbon-oxygen bond is formed determines the resulting selectivity, this step is most favorable on the spin 1 plane, which will be used for the following calculations. The various transition states leading to the different enantiomers can be formed by considering all possible approach vectors. The model complex used has a (1S,2S)-diaminocyclohexane backbone, as a probe reactant to find these approach vectors dihydronaphthalene was used.

## *2.2. Localizing the transition states that control the selectivity.*

The transition states were optimized with the gaussian09 package<sup>40</sup>, using the OPBE functional which consist of Handy's OPTX exchange<sup>41</sup> part and the well-known PBE<sup>42</sup> correlation part. This exchange-correlation combination has proven to be very performant for metal complexes with various spin states that are energetically close to each other<sup>43,44</sup>. These optimizations were done using a 6-311G Pople basis set. Starting from these initial guesses of the transition state, the distance of the forming C-O bond was fixed and a rotational scan was done around the Mn-O bond (Figure 4). The rotational scan is necessary to determine whether the original structure is the only transition state possible.

The minimum from the rotational scan was isolated and reoptimized using the same functional with a 6-31+G(d) basis set on C,H,N and O and a 6-311++G(2df,2p) for Mn and Cl, van der Waals contributions were added afterwards via Grimme's D3 corrections<sup>45</sup>.

For model (c) with the methylbenzene substituents, optimized geometries from the first step were modified directly without a prior rotational scan. Those structures were optimized directly on the high level. Frequency calculations were executed in order to calculate free energies at 295K using the

in-house software package, TAMkin.<sup>46</sup> A comparison of the free energies allows for the analysis of the enantioselectivity.

### 2.3. MOF synthesis

MIL-101(Cr) is synthesized according to a literature recipe<sup>32</sup> which differs from the original report by Ferey *et al.*<sup>31</sup> only by the omission of the use of hydrogen fluoride. This results in a significant decrease in surface area but still yields a good crystalline and porous material. 4 mmol of  $\text{Cr}(\text{NO}_3)_3 \cdot 9\text{H}_2\text{O}$  is mixed with 4 mmol of terphthalic acid and 20 ml of water in a teflon-lined steel autoclave. The autoclaves were heated to 210°C over two hours and then kept at that temperature for eight hours. Afterwards the autoclaves were allowed to naturally cool to room temperature. The resulting precipitation was filtered off on a membrane filter. A green powder remained on the filter together with a significant amount of needle-like crystals that point to unreacted terphthalic acid. The MOF was washed two times on the filter with 20 ml of DMF to wash away the bulk of remaining terphthalic acid. The remaining solid was then stirred at 60°C in DMF to wash out the last remaining acid. The solid was then again filtered off and dried under vacuum at 100°C. The powder XRD pattern of the result was in agreement with the reported pattern of MIL-101 and a Langmuir surface area of 2541 m<sup>2</sup>/g was calculated from nitrogen sorption.

### 2.4. Chloromethylation

In order to introduce an anchor point for further postmodification a chloromethylation reaction as proposed earlier by Goesten *et al.*<sup>47</sup> was used. 1 g of MIL-101 ( $\pm 1.3$  mmol) was suspended in 70 ml of nitromethane together with 7.8 mmol of  $\text{AlCl}_3 \cdot 6\text{H}_2\text{O}$  and 3.6 mmol of methoxyacetyl chloride. The suspension was stirred for 5 hours at 100°C under reflux cooling. The chloromethylated material was filtered off and washed with water at 60°C for 4h and DMF at 60°C for 4h. Compared to the original MIL-101 structure the DRIFT spectrum (Figure 9) shows a shoulder peak at 888 cm<sup>-1</sup> and a new peak at 919 cm<sup>-1</sup> the first can be attributed to trisubstituted benzene while the latter can be attributed to the H-C-H rocking vibration of the chloromethyl group. The powder showed a Langmuir surface area of 2479 m<sup>2</sup>/g, powder XRD showed no structural changes compared to the original material (Figure 11). The amount of chlorine was determined by XRF to be about 30% of the present terphthalic groups. A schematic representation of the modifications is shown in Figure 5.

### 2.5. Grafting 2,4,6-trihydroxybenzaldehyde

0.65g of chloromethylated MIL-101 ( $\pm 0.962$  mmol of chlorine) was brought in a schlenk flask together with 2.02 mmol of 2,4,6-trihydroxybenzaldehyde and 8.0 mmol of potassiumhydroxide and 0.1 mmol of 18-crown-6. The contents of the flask were then dried under vacuum for a short time at room temperature before placing it under an argon atmosphere. 10 ml of anhydrous DMF was added via a septum. The mixture was stirred at 95°C for 24h. Afterwards the solid was filtered and washed overnight with DMF at 60°C and two times with water at room temperature for three hours. The resulting powder showed a deep-red color instead of the original green color of the MIL-101(Cr). It was then dried under vacuum at 90°C. For the further steps it is vital that any potassium hydroxide is removed from the system. The Langmuir surface area was determined to be 2312 m<sup>2</sup>/g and the XRD pattern showed no structural changes (Figure 11). In the DRIFT spectrum (Figure 9) a new vibration at 1686 cm<sup>-1</sup> appears that can be assigned to an aldehyde C=O vibration.

### 2.6. Grafting (1R,2R)-(-)-1,2-cyclohexanediamine

0.5 g of the carrier with the first benzaldehyde moiety grafted ( $\pm 0.75$  mmol of benzaldehyde groups when assuming full conversion in the previous step) was suspended in 7.5 ml dioxane together with 5.6 mmol of (1R,2R)-(-)-1,2-cyclohexanediamine and 11.5 mmol of pyridine. The mixture was stirred under reflux conditions for 24 hours after filtration the red powder was washed two times with DMF for 3 h at room temperature and 1 time in water at 60°C overnight. It was then dried in vacuum at 90°C. DRIFT analysis (Figure 9) of the material showed two new peaks at 2852  $\text{cm}^{-1}$  and 2919  $\text{cm}^{-1}$ . The peak at 1686  $\text{cm}^{-1}$  is still present but has diminished. The Langmuir surface area was 2016  $\text{m}^2/\text{g}$  while powder XRD (Figure 11) showed the structure was preserved.

### 2.7. Grafting of 3,5-di-tert-salicylaldehyde

0.5 g of the material from the previous step was suspended in 7.5 ml of dioxane together with 1.14 mmol of 3,5-di-tert-butylbenzaldehyde and 11 mmol of pyridine. The suspension was stirred under reflux conditions for 24 hours after which the material was filtered off. The resulting red powder was washed two times overnight in water at 60°C and dried in vacuum at 80°C. The surface area was 1805  $\text{m}^2/\text{g}$  and the structure was unchanged as analysed via powder XRD (Figure 11). The DRIFT spectrum (Figure 9) shows the same distinct peaks as the previous step: 1686  $\text{cm}^{-1}$ , 2852  $\text{cm}^{-1}$  and 2919  $\text{cm}^{-1}$ .

### 2.8. Chelating manganese

0.4 g of salen ligand@MIL-101(Cr) and 0.5 mmol of manganese(II) acetate tetrahydrate was mixed in 16 ml DMF and refluxed for 24h. The filtered powder was stirred in 20 ml saturated aqueous NaCl solution. Afterwards the powder was washed in DMF at 60°C and acetone at room temperature. The material was dried in vacuum at 80°C. The manganese was quantified via XRF and shown to be 0.382 mmol/g. The Langmuir surface area was found to be 1418  $\text{m}^2/\text{g}$  and the structure remained virtually unchanged compared to the original MIL-101 system as shown by XRD analysis (Figure 11).

### 2.9. Catalytic test

20 mg of heterogeneous salen catalyst (0.0076 mmol of active sites) was mixed in 5 ml of dichloromethane in a 10 ml vial. 0.154 mmol of dihydronaphthalene was added together with 0.768 mmol N-methylmorpholine-N-oxide (NMO) 1 mmol of toluene was added as internal standard and 0.2 mmol 3-chloroperbenzoic acid was added in 2 equal steps. The system was left to stir for 2 hours at room temperature before the catalyst was filtered off. The product was analyzed with HPLC using a daicel AD-H column with a volumetric mixture of 98/2 hexane/isopropoxide with a flowrate of 0.9 ml/min as mobile phase. The detector was an UV-detector operating at 220nm. The catalyst was washed with dichloromethane and dried for two hours at 80°C and then reused for two more times with the same conditions. A blank reaction without any catalyst and with unmodified MIL-101 (using the same amount of chromium) was done under the same conditions.

### 3. Results and discussion

#### 3.1. Theoretical rationalization for the selectivity

The salen variant with *tert*-butyl groups on both sides leads to two possible approaches of the substrate with respect to the active complex, as we have reported before<sup>30</sup>. Rotational scans show that these are indeed the most stable transition states (Figure S1 of the supporting information). One leads to the (1R,2S)-enantiomer, the other to the (1S,2R)-enantiomer (shown in Figure 6). The specific bended shape of the salen complexes offers a clear cause for this selectivity. For the (1R,2S)-approach the substrate is sterically hindered by the wing of the salen complex facing upwards. The (1S,2R)-approach does not suffer from this unfavorable interaction and is thus found to be 10 kJ/mol more stable (Figure 6). The calculated energy difference is small, and should of course be treated with care. However, small energy differences are expected for different approaches in enantioselective reactions and thus this number is not surprising. Another difference between both approaches is the twist of the complex, an unfavorable approach pushes the wings down, inducing extra strain. This can be assessed by drawing a plane through the manganese and perpendicular to the manganese-oxygen bond. A measurement for the twist is the sum of the distance of the C5 and C5' carbon to this plane. For the favorable approach this distance is 3.69 Å, for the unfavorable (1R,2S)-approach this is 3.29 Å indicating the unfavorable approach pushes the wings of the complex open (Figure 7), contributing to the energy difference.

When grafting a salen complex covalently on a substrate an anchor point has to be introduced, in order to achieve this, the bulky groups on the 5 and/or 3 positions are often omitted for more reactive groups which are not necessarily on the same position. In order to simulate this, –OH groups were placed on one side of the complex on the 4 and 6 position, which corresponds to the grafting method we used to bind the complex to the support (Figure 5). When the substitutions on the salen complex are asymmetrical, the number of possible approaches of the substrate to the catalyst increases. For both enantiomers two possibilities exist, the first one has the –OH groups closest to the substrate. The second one has the groups on the opposite side. This leads to four possibilities in total. For the symmetrical salen complex with bulky groups the wing facing upwards blocks the (1R,2S)-approach with the aid of those substituents. When those groups on the ring facing upwards are the –OH groups, this approach is no longer blocked, effectively decreasing the selectivity as seen in the energy differences between the transition states (Figure 8). Most methods for constructing an asymmetric salen complex allow no control over which side of the ligand the non-bulky group are present on. Therefore the global selectivity will be lower as a combination of selective and less selective approaches will occur.

In order to further mimic the surroundings of the support a methylbenzene group was substituted on the hydroxyl group on the 4 position. This is only one of the possibilities how the complex can be grafted on the support, the substituent on the 6 position was not considered due to it being sterically less favorable. The results for this case are similar to the ones without the substitutions (Figure S4 of the supporting information), showing the methylbenzene groups are too far away to have any influence on the selectivity.

Looking at the structures in more detail (Figure 6) one can see the importance of the *tert*-butyl groups for the induction of enantioselectivity. Especially the substituents on the 3 and 3' positions seem crucial in blocking the (1R,2S)-approach. Once these groups are replaced by sterically less bulky –OH groups on the 4/6 positions the transition state for the less-favorable approach becomes unhindered. This is in agreement with the findings of Jacobsen *et al.*<sup>13</sup> who examined various substituents on the salen complex. The biggest part of the substrate, the aromatic ring in this case, interacts with the *tert*-butyl groups on the 3 position of the upward facing wing. The least-bulky part of the substrate also interacts with the complex via the *tert*-butyl group on the 3' position. However distances between the substrate and the upward facing wing are the smallest making this specific interaction the governing factor for enantioselectivity.

The substituents on the 5/5' positions are significantly less influential for the induction of selectivity which was also shown in experiments of Jacobsen *et al.*<sup>14</sup> The steric hindrance that blocks the (1R,2S)-approach is relatively small, with a distance of only 3.58 Å compared to less than 3 Å for the interaction with the *tert*-butyl group on the 3 position. This can imply there are two separate effects at work in inducing the selectivity. The transition state selectivity is the first effect, this is guided for the most by the 3 and 3' substituents. The transition state effect is crucial since the absence of these substituents leads to a non-selective catalyst. The second effect is probably the approach of the substrate towards the activated oxygen. The path followed by a reactant molecule to reach the active site and the orientation of this molecules is also managed by the ligand and the substituents present. Since the 5 and 5' groups have only a small influence on the transition state selectivity but experimental observations show they do have an effect on the resulting enantioselectivity they will probably manage the orientation of the approach.

Similar to the symmetrical salen complex the shape of the asymmetrical complex for the different transition states can be correlated to the stability of the approach (Table 2). This effect is also a consequence of the steric hindrance, if the complex is 'pushed' open the transition state is less stable. Table 2 shows the comparison between the C5/C5' out of plane displacement and the relative free energy of the transitions states. When comparing the geometry of a transition state for different enantiomers both the substrate-ligand distance and the twist of the complex have to be taken into account to assess the possibilities of approach.

Until now we have focused on the influence of the steric effects on the enantioselectivity of the material, but the modification of substituents also has some electronic effects. To assess these effects different groups of similar size with different electron withdrawing and donating effects have to be compared. Although the asymmetric catalyst with methylbenzene substituents on the –OH modification is more bulky than the variant without those substituents, we showed before that for dihydronaphthalene this group is too far away from the active site to have any steric effect. Thus the only effects at work here are electron donating effects. The electron donating power of an ether is slightly lower as for an alcohol, which slightly decreases the selectivity. But this conclusion has to be drawn with care since the energy difference is barely 1 kJ/mol (figure S4 of the supporting information). This allows us to conclude the steric effects are significantly more important than the electronic effects. That conclusion is in agreement with an experimental study from Jacobsen *et al.*<sup>48</sup> where strongly electron donating groups on the C5/C5' positions yielded a slight improvement of the enantioselectivity. These electronic effects have shown to have a much more pronounced effect on the activity of the catalyst as studied by Kochi *et al.*<sup>36</sup> but this is beyond the scope of our report.

### 3.2. Selectivity of asymmetric grafted complexes

To confirm the decrease in selectivity with asymmetrical complexes we have immobilized the salen complex via a reported procedure on an alternative substrate, the MIL-101(Cr) metal organic framework. The MIL-101(Cr) MOF is a very stable material, both thermally as in most common solvents. However its use as a carrier material for catalytically active sites is severely limited by the lack of any functional groups available for postmodification. The chloromethylation procedure proposed by Goesten *et al.*<sup>47</sup> is an excellent way to solve this. The procedure is relatively mild, and is applicable to structures which are far less stable than the proposed material. The primary chlorine moiety is a good leaving group for further modifications.

The Jacobsen salen complex was systematically build up as shown in Figure 5 and followed by various characterization techniques. All reactions have been analyzed by DRIFT measurements (Figure 9). The chloromethylation is characterized by some slightly visible absorption peaks around  $900\text{ cm}^{-1}$ . The coupling of 2,4,6-trihydroxybenzaldehyde is observed by the presence of a C=O stretching vibration at  $1686\text{ cm}^{-1}$ . The presence of this peak after thorough washing is shows that the benzaldehyde is grafted on the structure. The next step, involving the formation of the first imine bond, coupling (1R,2S)-diaminocyclohexane is shown by two peaks at  $2852\text{ cm}^{-1}$  and  $2919\text{ cm}^{-1}$  corresponding to the hydrogen vibrations of the cyclohexane moiety. A broad peak around  $1633\text{ cm}^{-1}$  could point to the formation of the C=N bond but it is only slightly visible. The further steps featuring the formation of a second imine bond grafting 3,5-di-tert-butylbenzaldehyde and the chelating of manganese does not lead to any new vibrations.

The successful chelating of manganese is determined by XRF analysis, after washing the final material several times the manganese was still present and could be quantified at  $0.38\text{ mmol/g}$ . This is a relatively high loading, indicating there will probably be complexes both in the pores and on the outer surface of the MOF. When employing a postmodification procedure on a metal organic framework the structural integrity of the host should be assessed at every step. The way to confirm this is verifying the crystallinity of the sample. This is achieved by a powder XRD measurement after every step (Figure 11). These show the original crystallinity remains during the grafting steps, thus the structural integrity of the host is maintained.

The catalytic activity of the immobilized salen complex is assessed by a test reaction. For that we selected the epoxidation of dihydronaphthalene, which is a widely used benchmark reaction for the system<sup>12,49-51</sup>. The use of 3-chloroperbenzoic acid and 4-Methylmorpholine N-oxide has shown to be performant in combination with manganese salen complexes. In our hands the commercial salen catalyst gave a conversion of 85% and 70% enantiomeric excess. The proposed catalyst showed a conversion of 48% with a %ee of 62.5%. The conversion is significantly lower compared to the commercial Jacobsen complex in homogeneous conditions, which yielded a conversion of approximately 85%. The selectivity is also lower; which has been observed in similar grafting procedures on other carrier materials<sup>28,29,33,52,53</sup>. Some alternative immobilization procedures such as electrostatic grafting and encapsulation have shown to maintain the original selectivity as we have

shown in earlier reports<sup>30,35</sup>. However we can still conclude this metal organic framework is a good carrier for the covalent grafting since the loss of selectivity is very limited.

To verify the reusability of the crafted catalyst two consecutive runs were executed using the same batch. During these runs the selectivity remained the same, while the conversion decreased significantly. However when comparing the turn over number (TON) for the different runs it remains virtually unchanged (Figure 12). Meaning the decrease in activity is mostly due to the loss of material in the washing and drying steps between the runs. This shows the complex is firmly grafted to the MIL-101 host structure and there is minimal leaching of the active sites. The same is shown by the lack of any detectible amount of manganese present in the reaction mixture. These results confirm the conclusions from the ab initio modelling, the grafting of the asymmetric complex decreases the selectivity compared to a reaction in the homogeneous phase with the symmetrical complex.

### Conclusions

By using the full salen complex as a model and dihydronaphthalene as a probe substrate we were able to obtain insight in the selectivity of the manganese-salen complex in the epoxidation of unfunctionalized olefins. It can be shown that there is one optimal geometry for each enantioselective approach, rotational scans on the transition state show only one minimum for the (1R,2S) and (1S,2R) structure. The transition states provide a rationale for the experimental observed dependence of the selectivity with respect to the type and place of substituents on the ligand. The 3/3' positions are the most crucial and they induce the most significant interaction with the approaching substrate. Substituents on the 5/5' position are less crucial and will probably manage the orientation of the approach rather than the actual transition state. A second geometrical effect is the shape of the complex, an unfavorable approach pushes the complex in a more flattened geometry while the favorable approach allows the complex more freedom to form its folded orientation. These results allow us to propose a rationale for the best method of immobilizing salen-type complexes, since covalent grafting will always lead to some decrease in selectivity. Alternative approaches such as electrostatic immobilization and encapsulation are much more promising.

Many approaches for heterogenizing a salen complex require the use of an asymmetric complex on which the more bulky groups are replaced by a more reactive group that can couple to the carrier. The models of asymmetric complexes show the energy difference in the transition state for the (1S,2R)- and (1R,2S)-approach is significantly smaller than for the symmetric complex with *tert*-butyl substitutions that were taken as a reference. Therefore the grafted asymmetric complexes are prone to be less selective than the homogeneous ones. As an example of covalent grafting we applied a well-established postmodification procedure on an alternative substrate, the MIL-101(Cr) metal organic framework. Compared to the homogeneous catalyst, this systems still yields a very selective catalyst showing MIL- 101(Cr) is a good carrier material for the salen complex.

In order to design a heterogeneous salen catalyst with a minimal loss of selectivity a less-invasive grafting procedure should be used. Possible approaches are electrostatic grafting where the support material is charged and acts as a counter ion on the axial position of the salen complex<sup>35,53</sup>. Another approach is the encapsulation of the complex in the cages of the support material confining it by sufficiently small window sizes, as shown earlier by these authors<sup>30</sup>.

### Acknowledgements

The research was financed by UGent GOA grant 01G00710, the European Research Council for funding through the European Community's Seventh Framework Programme (FP7(2007-2013) ERC grant agreement no. \ 240483) and the Research Board of Ghent University (BOF). S.W. acknowledges Research Foundation Flanders for a fellowship. Computational resources and services were provided by Ghent University (*Stevin Supercomputer Infrastructure*).

## References

- (1) Breuer, M.; Ditrach, K.; Habicher, T.; Hauer, B.; Keßeler, M.; Stürmer, R.; Zelinski, T. *Angewandte Chemie International Edition* **2004**, *43*, 788.
- (2) Hawkins, J. M.; Watson, T. J. N. *Angewandte Chemie International Edition* **2004**, *43*, 3224.
- (3) Blaser, H. U.; Spindler, F.; Studer, M. *Applied Catalysis A: General* **2001**, *221*, 119.
- (4) Gao, Y.; Hanson, R. M.; Klunder, J. M.; Ko, S. Y.; Masamune, H.; Sharpless, K. B. *J. Am. Chem. Soc.* **1987**, *109*, 5765.
- (5) Carlier, P. R.; Sharpless, K. B. *J. Org. Chem.* **1989**, *54*, 4016.
- (6) Deubel, D. V.; Frenking, G.; Gisdakis, P.; Herrmann, W. A.; Rosch, N.; Sundermeyer, J. *Accounts Chem. Res.* **2004**, *37*, 645.
- (7) Jorgensen, K. A.; Wheeler, R. A.; Hoffmann, R. *J. Am. Chem. Soc.* **1987**, *109*, 3240.
- (8) Katsuki, T.; Sharpless, K. B. *J. Am. Chem. Soc.* **1980**, *102*, 5974.
- (9) Sharpless, K. B.; Woodard, S. S.; Finn, M. G. *Pure Appl. Chem.* **1983**, *55*, 1823.
- (10) Woodard, S. S.; Finn, M. G.; Sharpless, K. B. *J. Am. Chem. Soc.* **1991**, *113*, 106.
- (11) Katsuki, T. *J. Synth. Org. Chem. Jpn.* **1995**, *53*, 940.
- (12) Irie, R.; Noda, K.; Ito, Y.; Matsumoto, N.; Katsuki, T. *Tetrahedron Lett.* **1990**, *31*, 7345.
- (13) Zhang, W.; Jacobsen, E. N. *J. Org. Chem.* **1991**, *56*, 2296.
- (14) Jacobsen, E. N.; Zhang, W.; Muci, A. R.; Ecker, J. R.; Deng, L. *J. Am. Chem. Soc.* **1991**, *113*, 7063.
- (15) Lee, N. H.; Muci, A. R.; Jacobsen, E. N. *Tetrahedron Lett.* **1991**, *32*, 5055.
- (16) Palucki, M.; McCormick, G. J.; Jacobsen, E. N. *Tetrahedron Lett.* **1995**, *36*, 5457.
- (17) Fristrup, P.; Dideriksen, B. B.; Tanner, D.; Norrby, P. O. *J. Am. Chem. Soc.* **2005**, *127*, 13672.
- (18) Cavallo, L.; Jacobsen, H. *Angewandte Chemie International Edition* **2000**, *39*, 589.
- (19) Jacobsen, H.; Cavallo, L. *Chemistry – A European Journal* **2001**, *7*, 800.
- (20) Cavallo, L.; Jacobsen, H. *Inorg. Chem.* **2004**, *43*, 2175.
- (21) Abashkin, Y. G.; Burt, S. K. *Org. Lett.* **2004**, *6*, 59.
- (22) Linde, C.; Arnold, M.; Norrby, P. O.; Akermark, B. *Angew. Chem.-Int. Edit. Engl.* **1997**, *36*, 1723.
- (23) Norrby, P. O.; Linde, C.; Akermark, B. *J. Am. Chem. Soc.* **1995**, *117*, 11035.
- (24) Cavallo, L.; Jacobsen, H. *Eur. J. Inorg. Chem.* **2003**, 892.
- (25) Cavallo, L.; Jacobsen, H. *J. Org. Chem.* **2003**, *68*, 6202.
- (26) Khavrutskii, I. V.; Musaev, D. G.; Morokuma, K. *Proceedings of the National Academy of Sciences of the United States of America* **2004**, *101*, 5743.
- (27) Canali, L.; Sherrington, D. C.; Deleuze, H. *React. Funct. Polym.* **1999**, *40*, 155.
- (28) Angelino, M. D.; Laibinis, P. E. *Macromolecules* **1998**, *31*, 7581.
- (29) Angelino, M. D.; Laibinis, P. E. *Journal of Polymer Science Part A: Polymer Chemistry* **1999**, *37*, 3888.
- (30) Bogaerts, T.; Van Yperen-De Deyne, A.; Liu, Y.-Y.; Lynen, F.; Van Speybroeck, V.; Van Der Voort, P. *Chem. Commun.* **2013**, *49*, 8021.
- (31) Ferey, G.; Mellot-Draznieks, C.; Serre, C.; Millange, F.; Dutour, J.; Surble, S.; Margiolaki, I. *Science* **2005**, *309*, 2040.
- (32) Jiang, D.; Burrows, A. D.; Edler, K. J. *CrystEngComm* **2011**.
- (33) Das, P.; Silva, A. R.; Carvalho, A. P.; Pires, J.; Freire, C. *Catal. Lett.* **2009**, *129*, 367.
- (34) Ji, R. N.; Yu, K.; Lou, L. L.; Gu, Z. C.; Liu, S. X. *J. Inorg. Organomet. Polym. Mater.* **2010**, *20*, 675.
- (35) De Decker, J.; Bogaerts, T.; Muylaert, I.; Delahaye, S.; Lynen, F.; Van Speybroeck, V.; Verberckmoes, A.; Van der Voort, P. *Mater. Chem. Phys.* **2013**, *141*, 967.
- (36) Srinivasan, K.; Michaud, P.; Kochi, J. K. *J. Am. Chem. Soc.* **1986**, *108*, 2309.

- (37) Plattner, D. A.; Feichtinger, D.; El-Bahraoui, J.; Wiest, O. *Int. J. Mass Spectrom.* **2000**, *195*, 351.
- (38) Abashkin, Y. G.; Collins, J. R.; Burt, S. K. *Inorg. Chem.* **2001**, *40*, 4040.
- (39) Wouters, S.; Bogaerts, T.; Van der Voort, P.; Van Speybroeck, V.; Van Neck, D. *J. Chem. Phys.* **2014**, *140*, 241103.
- (40) M. J. Frisch, G. W. T., H. B. Schlegel, G. E. Scuseria, M. A. Robb, J. R. Cheeseman, G. Scalmani, V. Barone, B. Mennucci, G. A. Petersson, H. Nakatsuji, M. Caricato, X. Li, H. P. Hratchian, A. F. Izmaylov, et al.; Revision B.01, Gaussian, Inc., Wallingford CT ed. 2009.
- (41) Handy, N. C.; Cohen, A. J. *Mol. Phys.* **2001**, *99*, 403.
- (42) Perdew, J. P.; Burke, K.; Ernzerhof, M. *Phys. Rev. Lett.* **1996**, *77*, 3865.
- (43) Swart, M. *Inorg. Chim. Acta* **2007**, *360*, 179.
- (44) Swart, M.; Groenhof, A. R.; Ehlers, A. W.; Lammertsma, K. *J. Phys. Chem. A* **2004**, *108*, 5479.
- (45) Grimme, S.; Antony, J.; Ehrlich, S.; Krieg, H. *J. Chem. Phys.* **2010**, *132*.
- (46) Ghysels, A.; Verstraelen, T.; Hemelsoet, K.; Waroquier, M.; Van Speybroeck, V. *J. Chem. Inf. Model.* **2010**, *50*, 1736.
- (47) Goesten, M. G.; Sai Sankar Gupta, K. B.; Ramos-Fernandez, E. V.; Khajavi, H.; Gascon, J.; Kapteijn, F. *CrystEngComm* **2012**, *14*, 4109.
- (48) Chang, S.; Heid, R. M.; Jacobsen, E. N. *Tetrahedron Lett.* **1994**, *35*, 669.
- (49) Zhang, W.; Loebach, J. L.; Wilson, S. R.; Jacobsen, E. N. *J. Am. Chem. Soc.* **1990**, *112*, 2801.
- (50) Yamada, T.; Imagawa, K.; Nagata, T.; Mukaiyama, T. *Chem. Lett.* **1992**, 2231.
- (51) Irie, R.; Noda, K.; Ito, Y.; Matsumoto, N.; Katsuki, T. *Tetrahedron: Asymmetry* **1991**, *2*, 481.
- (52) Kuzacuteniarska-Biernacka, I.; Pereira, C.; Carvalho, A. P.; Pires, J.; Freire, C. *Appl. Clay Sci.* **2011**, *53*, 195.
- (53) Maia, F.; Mahata, N.; Jarrais, B.; Silva, A. R.; Pereira, M. F. R.; Freire, C.; Figueiredo, J. L. *J. Mol. Catal. A-Chem.* **2009**, *305*, 135.

Figure Captions

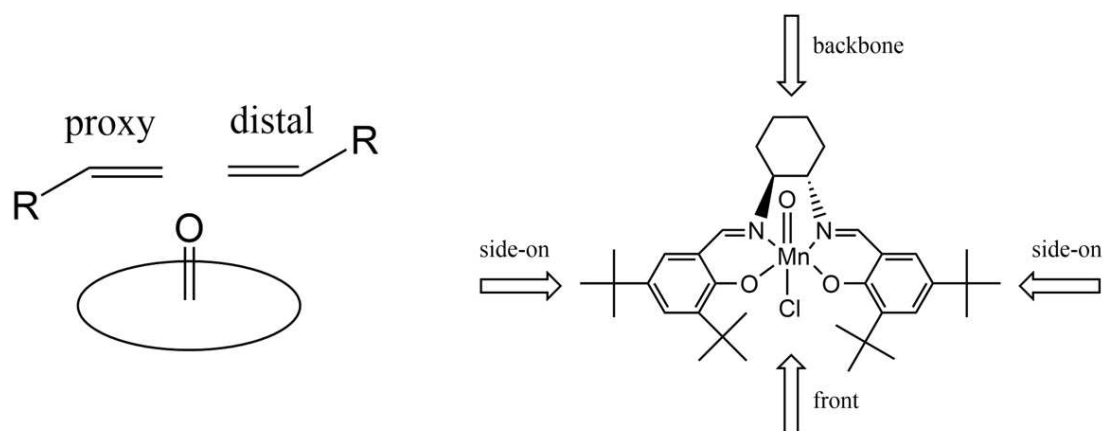


Figure 1. schematic representation of various approach vectors to the salen complex, adapted from Frstrup *et al.*<sup>17</sup> and Jacobsen *et al.*<sup>19</sup>

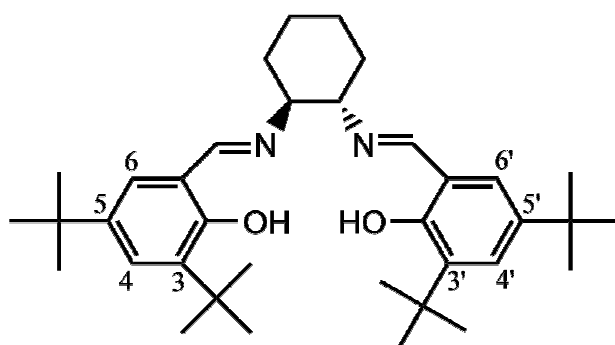


Figure 2. symmetrical salen ligand with a diamine backbone and the numbering of the substituents.

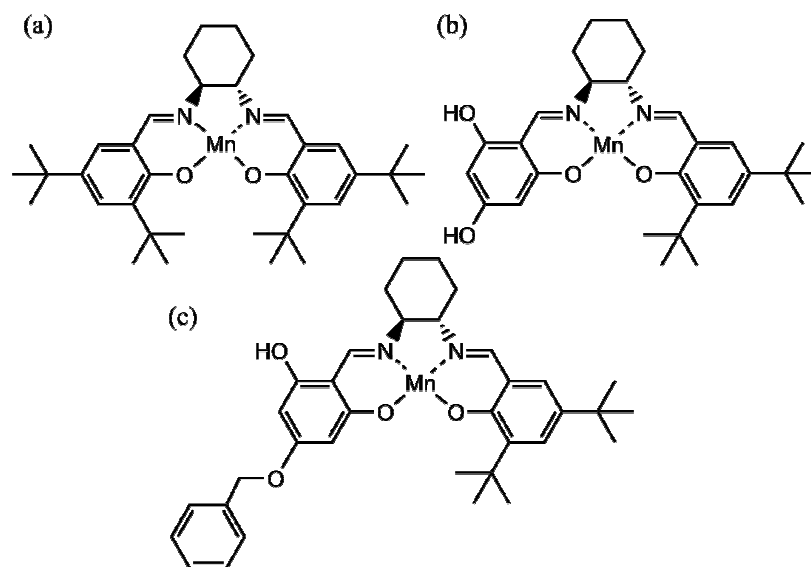


Figure 3. Different models used in this study

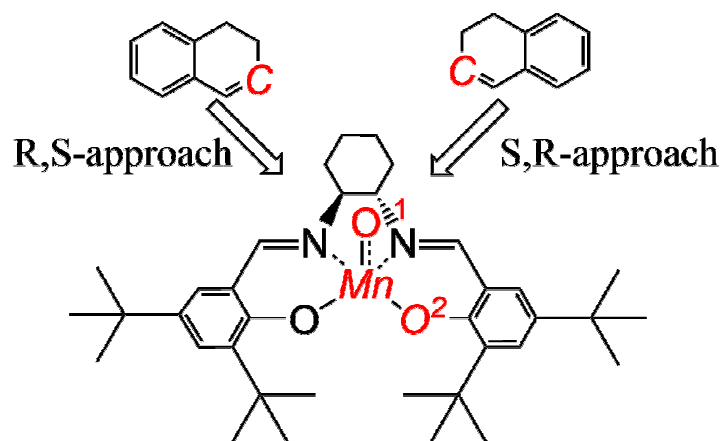


Figure 4. Rotational scans were done over the C-O<sup>1</sup>-Mn-O<sup>2</sup> dihedral angle of the transition state geometry as indicated.

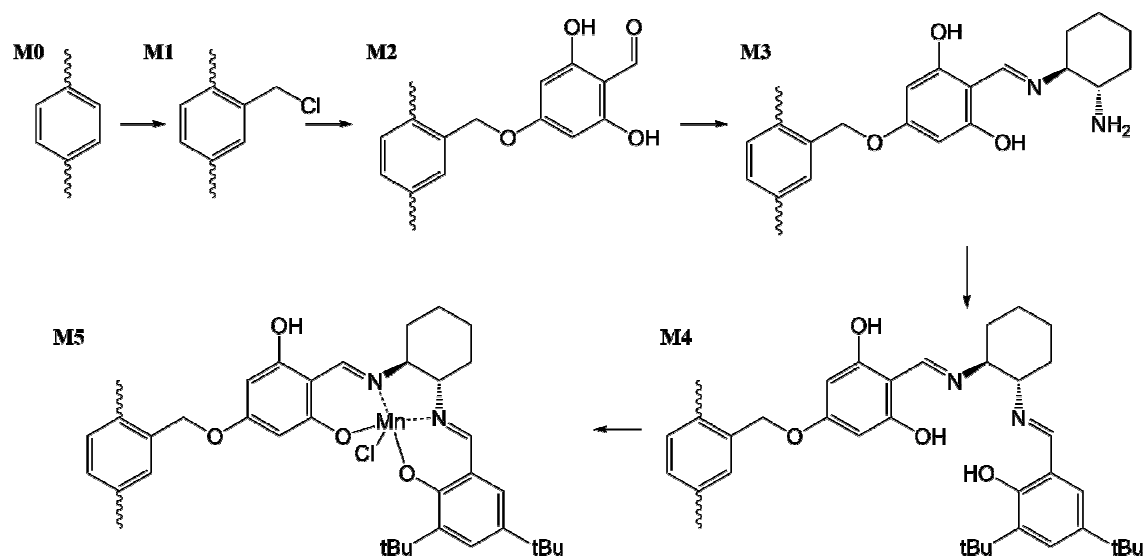


Figure 5. Different steps in the build-up of the complex on a terephthalic linker of the MIL-101 metal organic framework

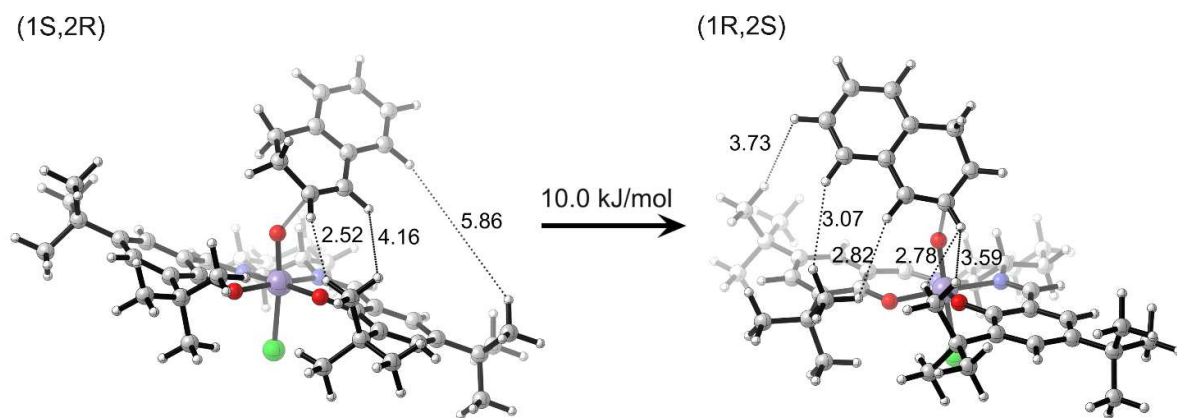


Figure 6. most stable transition state for the (1S,2R)-approach and the (1R,2S)-approach for model (a). The steric hindrance for the latter is significantly larger leading to it being 10 kJ/mol lower in free energy (distances in ångström).

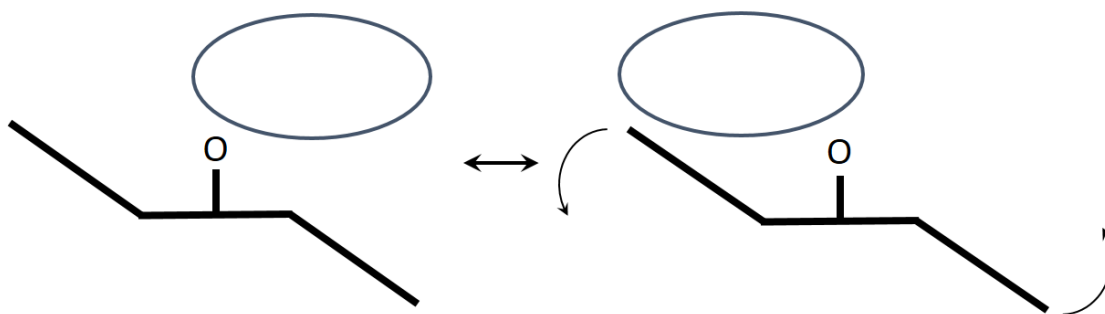


Figure 7. Schematic representation of the change in the twist of the complex for the different approaches.

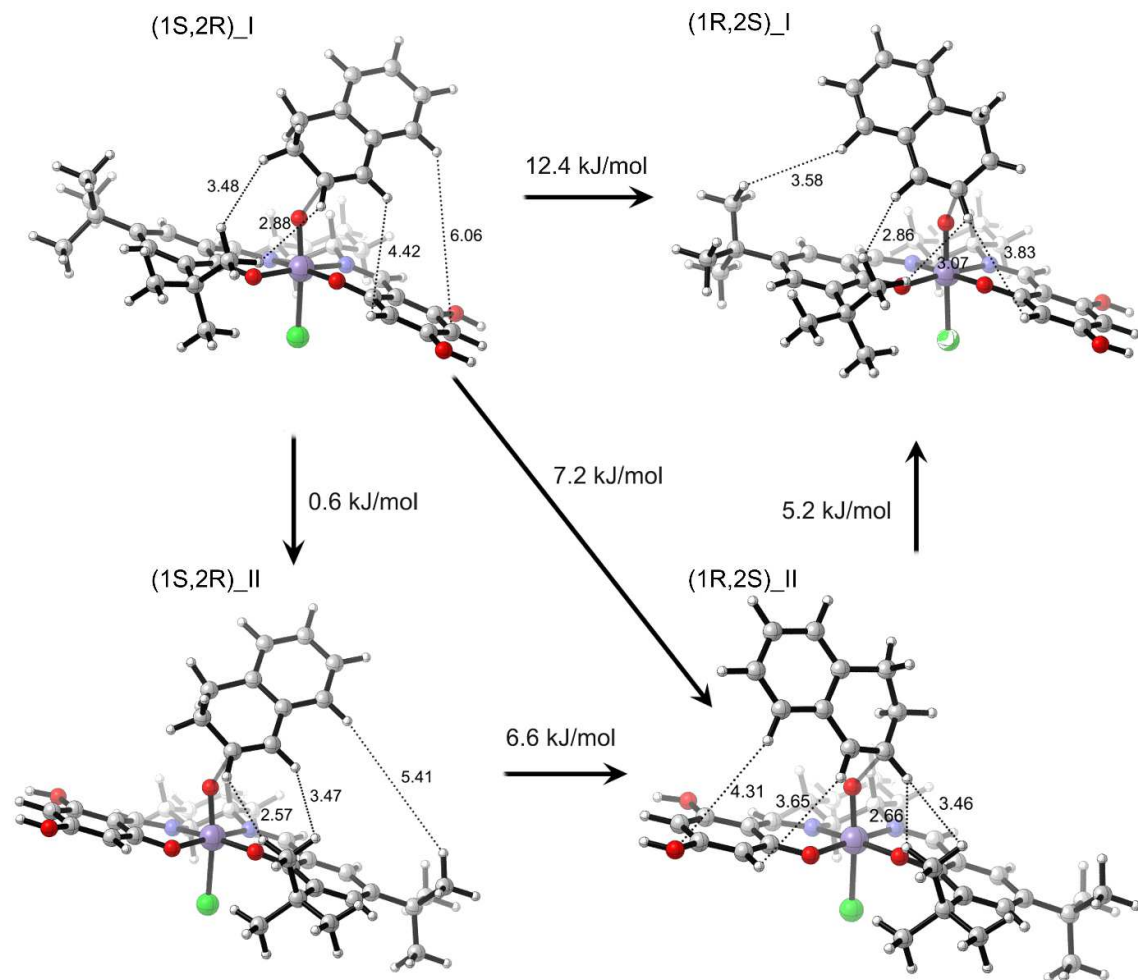


Figure 8. Different transition states for the asymmetric salen complex with hydroxy-groups (model (b)). The two possible positions of the groups are denoted I and II, (1S,2R)<sub>I</sub> is the most stable (distances in ångström).

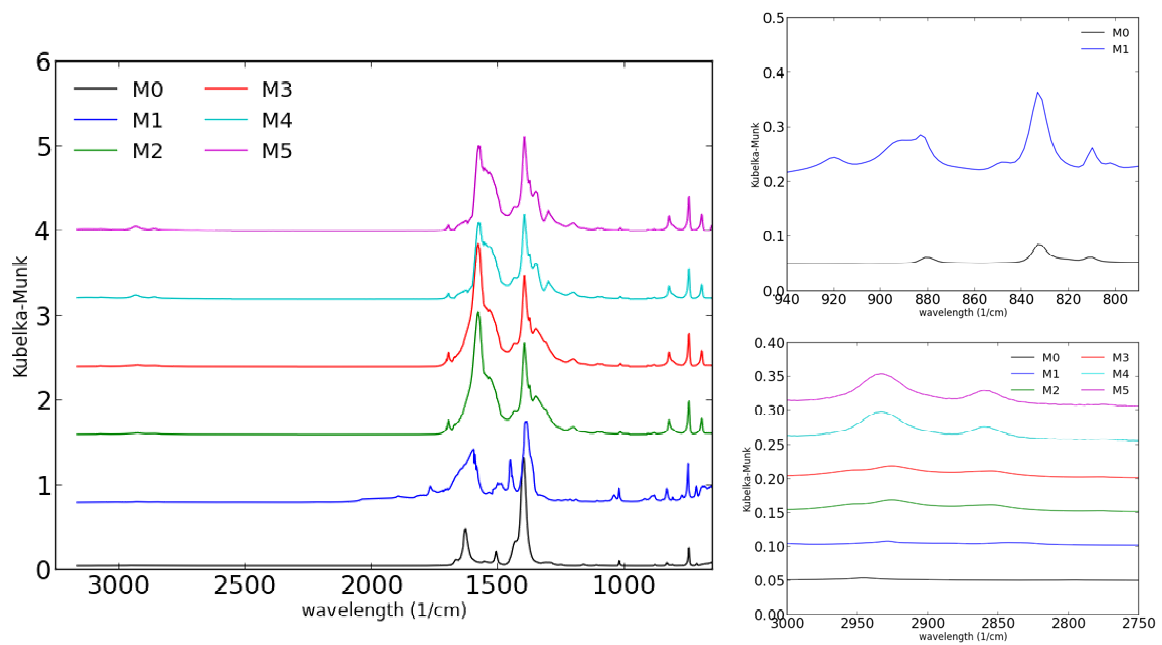


Figure 9. Evolution of the IR pattern during the postmodification steps

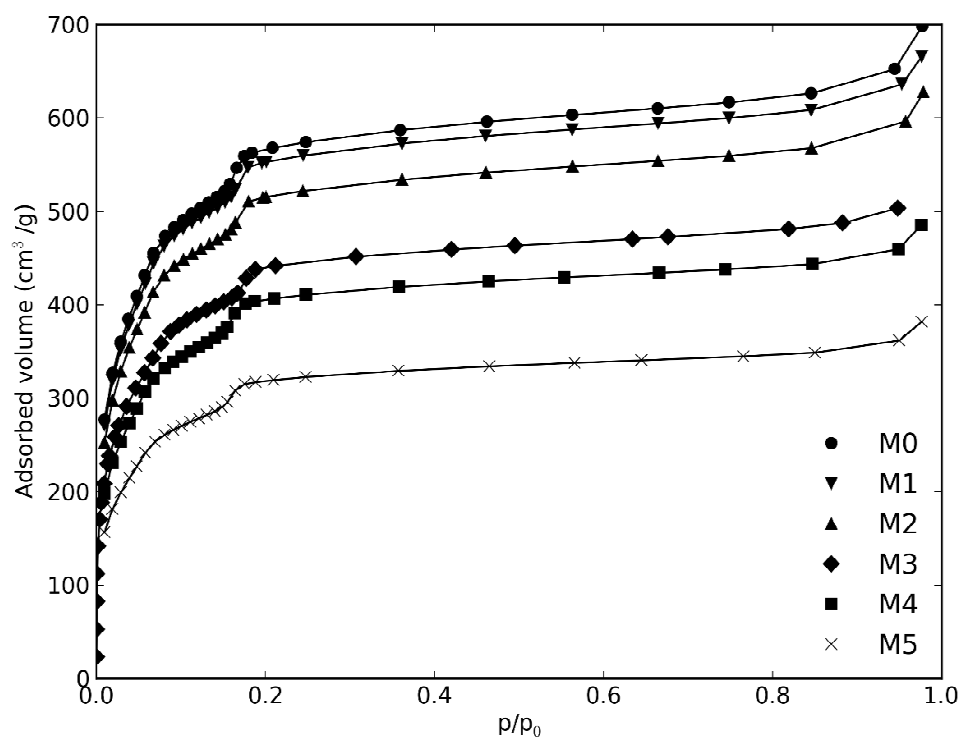


Figure 10. Evolution of the nitrogen sorption for the different steps in the construction of the complex (M0 - M5).

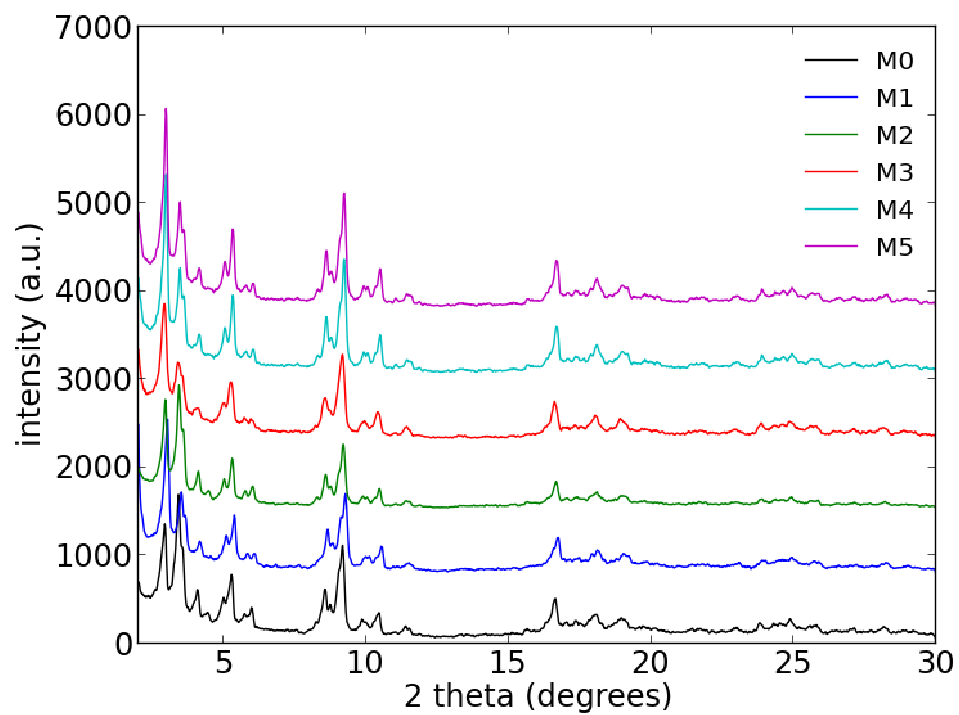


Figure 11. Evolution of the XRD pattern during the postmodification steps (M0-M5).

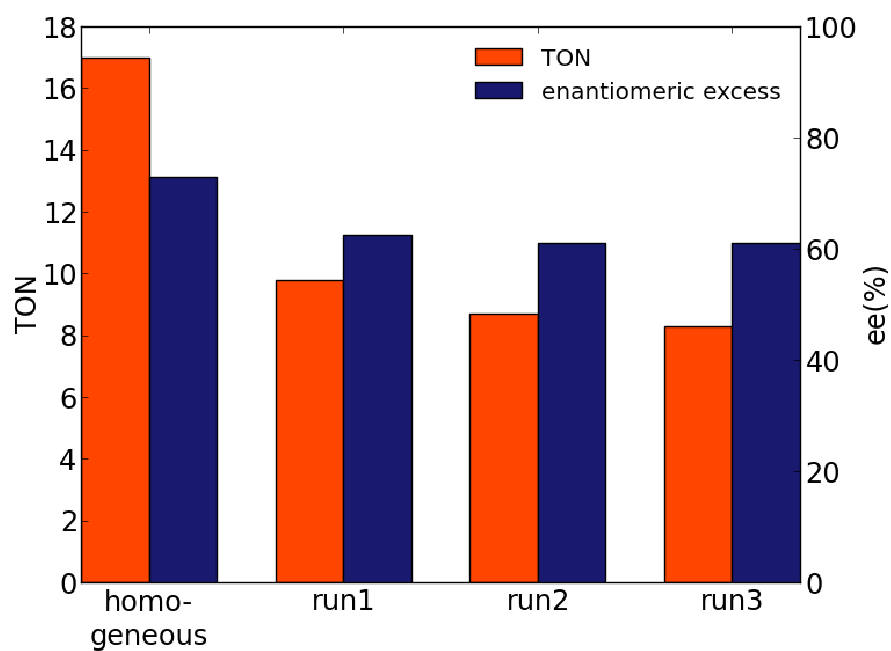
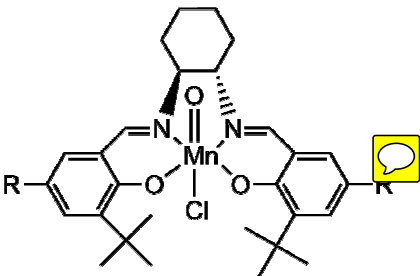
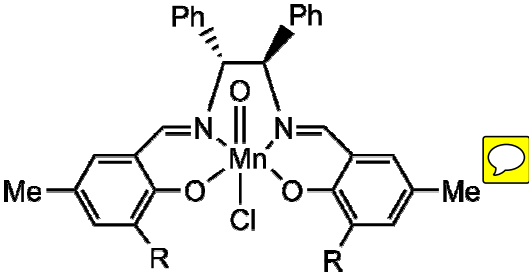


Figure 12. Turn over numbers and selectivities for the various runs using the homogeneous, symmetrical complex and the grafted, asymmetrical complex.

## Tables

Table 1. Selectivity of salen-type catalysts bearing different substitutions in the epoxidation of methylstyrene.<sup>13,14</sup>

Catalyst	Substituents	%ee
	R = Me  R = <i>tert</i> -butyl	80%  92%
	R = H  R = <i>tert</i> -butyl	0% - 3%  81%

*Table 2. Comparison of the complex shape to the selectivity.*

	Vertical C5/C5' distance (Å)	Relative transition state free energy at 293K (kJ/mol)
(1S,2R)_I	3.559	0
(1S,2R)_II	3.335	0.6
(1R,2S)_I	2.138	12.4
(1R,2S)_II	2.877	7.2